J Mater Sci (2009) 44:5225–5234
DOI 10.1007/s10853-009-3663-9

FERROELECTRICS

Field-induced inter-ferroelectric phase transformations and domain mechanisms in high-strain piezoelectric materials: insights from phase field modeling and simulation

Yu U. Wang

Received: 16 March 2009 / Accepted: 2 June 2009 / Published online: 18 June 2009

Abstract Large, reversible and anhysteretic strain induced by external field is desired for multifunctional materials used in sensors, actuators and transducers. However, these desired attributes usually compromise each other, leading to trade-offs in materials' properties and limiting their applicability. This paper focuses on field-induced inter-ferroelectric phase transformations. Some fundamental principles and domain mechanisms are systematized based on insights learned from phase field modeling and simulations, whose synergistic operations are expected to provide unique combination of large, reversible, and anhysteretic strain attributes. These working principles are: (i) Field-induced inter-ferroelectric structural phase transformation to achieve large strain; (ii) Field-induced stable-metastable phase transformation to maximize reversibility; (iii) Heterogeneous nucleation-and-growth process at domain walls to enhance low-field responses; (iv) Deactivation of domain wall motion by applying external fields along nonpolar axes to minimize hysteresis; (v) Domain wall broadening mechanism and domain size effect to exploit nanoscale engineered domain microstructures; and (vi) Bridging domain mechanism and phase coexistence to promote ferroelectric shape memory effects. It is shown that special initial domain microstructures and preferred evolution kinetic pathways can be achieved by crystallographic domain engineering technique, which allow multiple principles to work together without compromising one another. Due to the commonalities and fundamental interrelations among ferroelectric, ferromagnetic and ferroelastic materials, the gained understanding of thermodynamic and kinetic principles has general implications to displacive phase transformations in ferroic materials and is helpful for design of new functional materials with advanced field-induced strain properties.

Y. U. Wang (✉)
Department of Materials Science and Engineering,
Michigan Tech, Houghton, MI 49931, USA
e-mail: wangyu@mtu.edu

Introduction

Large, reversible and anhysteretic strain produced in response to external electric, magnetic, mechanical, and/or thermal stimuli is one of the essential requirements for multifunctional materials in sensor, actuator and transducer applications. Phase transforming materials (ferroics and multiferroics) are the best choice: crystallographic structural transformations offer the desired large spontaneous strain, their ferroic nature provides a convenient handle to control the phase transformation and select orientation/polar variants by external fields, and the displacive (diffusionless) phase transitions give rapid response to external stimuli. Unfortunately, the desired attributes of large, reversible and anhysteretic strain responses usually compromise each other: while the conventional mechanisms of structural phase transformation, domain switching, and domain wall motion produce large strain, such strain is impaired by large hysteresis or irreversibility; on the other hand, the intrinsic response of single-phase, single-domain ferroic materials is hysteresis-free, but the strain is small. Such trade-offs impose serious limitations on the materials' applicability. In fact, as reflected in macroscopic behaviors, ferroics, i.e., ferroelastics, ferroelectrics, and ferromagnetics, are characterized, respectively, by elastic (strain–stress), electric (polarization–electric field) and magnetic (magnetization–magnetic field) hysteresis, which originate from the underlying domain switching processes.

Therefore, eliminating hysteresis while retaining other desirable attributes of ferroic materials pose challenges.

In this study, we tackle these challenging issues by exploring favorable kinetic pathways for domain evolutions during inter-ferroic phase transformations. Phase field modeling and simulation are employed to investigate the domain microstructures and mechanisms for achieving unique combination of desired attributes of large, reversible and anhysteretic strain responses. To be specific, we will focus on ferroelectric materials and show that engineering of domain microstructure formation and control of domain evolution pathway during inter-ferroelectric phase transformation provide effective means to exploit the desired piezoelectric strain properties. Based on the commonalities and fundamental interrelations among ferroelectric, ferromagnetic, and ferroelastic materials, the insights and conclusions obtained from ferroelectrics also provide useful implications to other ferroic materials.

Phase field model of ferroelectrics

A ferroelectric system is, in general, structurally, electrically, and compositionally (for solid solutions) heterogeneous, which could be a polycrystal consisting of multiple grains, phases, and domains. The polycrystalline grain structure is described by a grain rotation matrix field $R_{ij}(\mathbf{r})$, which describes the geometry (size, shape, location) and crystallographic orientation of individual grains [1, 2]. A single crystal corresponds to a special case of a polycrystal with $R_{ij}(\mathbf{r}) = \delta_{ij}$ (i.e., identity matrix) independent of spatial position $\mathbf{r}$, where δ_{ij} is Kronecker delta symbol. The composition distribution is described by a scalar field $x(\mathbf{r})$, which describes the molar fraction of one component, e.g., $PbTiO_3$ in $Pb(Zr_{1-x}Ti_x)O_3$ pseudo-binary solid solution. In compositionally homogeneous solid solutions or compounds (e.g., $BaTiO_3$), $x(\mathbf{r}) = \text{const}$. The domain microstructure is described by polarization field $\mathbf{P}(\mathbf{r})$. The polarization direction in each domain defines the ferroelectric phase state of individual domains. The total free energy of such a ferroelectric system under external electric field $\mathbf{E}^{\text{ex}}$ is [2–6]:

$$F = \int d^3r \left[f\left(x, R_{ij}P_j\right) + \frac{\beta_P}{2}\frac{\partial P_i}{\partial r_j}\frac{\partial P_i}{\partial r_j} + \frac{\beta_x}{2}\frac{\partial x}{\partial r_k}\frac{\partial x}{\partial r_k} - P_k E_k^{\text{ex}} \right] + \frac{1}{2}\int \frac{d^3k}{(2\pi)^3}\left[\frac{n_i n_j}{\varepsilon_0}\tilde{P}_i\tilde{P}_j^* + K_{ijkl}\tilde{\varepsilon}_{ij}^0\tilde{\varepsilon}_{kl}^{0*} \right], \quad (1)$$

where summation convention over repeated indices is implied.

The function $f(x, \mathbf{P})$ is the nonequilibrium local bulk free energy density that defines the thermodynamic properties of ferroelectric phases in stress-free homogeneous states, which can be approximated as a sum of $\mathbf{P}$-dependent and $\mathbf{P}$-independent energy contributions [7]:

$$f(x, \mathbf{P}) = f_{\text{LGD}}(x, \mathbf{P}) + f_{\text{RS}}(x). \quad (2)$$

The $\mathbf{P}$-dependent function $f_{\text{LGD}}(x, \mathbf{P})$ is formulated by Landau–Ginzburg–Devonshire (LGD) theory [8]:

$$\begin{aligned} f_{\text{LGD}}(\mathbf{P}) =& \alpha_1\left(P_1^2 + P_2^2 + P_3^2\right) + \alpha_{11}\left(P_1^4 + P_2^4 + P_3^4\right) \\ &+ \alpha_{12}\left(P_1^2P_2^2 + P_2^2P_3^2 + P_3^2P_1^2\right) \\ &+ \alpha_{111}\left(P_1^6 + P_2^6 + P_3^6\right) + \alpha_{112}\Big[P_1^4\left(P_2^2 + P_3^2\right) \\ &+ P_2^4\left(P_3^2 + P_1^2\right) + P_3^4\left(P_1^2 + P_2^2\right)\Big] + \alpha_{123}P_1^2P_2^2P_3^2, \end{aligned} \quad (3)$$

where the polynomial expansion coefficients α_i, α_{ij}, and α_{ijk} are functions of temperature T and composition x [8, 9]. Note that $\mathbf{P}$ in LGD polynomial in Eq. 3 is defined with respect to a local coordinate system aligned with $\langle 100 \rangle$ crystallographic axes of individual grain lattices, while in Eq. 1 $\mathbf{P}$ is defined with respect to a global coordinate system attached to the polycrystalline sample. The operation $R_{ij}P_j$ in the function $f(x, R_{ij}P_j)$ in Eq. 1 transforms $\mathbf{P}(\mathbf{r})$ from global sample system to local crystallographic system in each grain [2]. The $\mathbf{P}$-independent function $f_{\text{RS}}(x)$ is formulated by regular solution theory [7]

$$f_{\text{RS}}(x) = \frac{w}{2}x(1-x) + \frac{k_{\text{B}}T}{\Omega}[x\ln x + (1-x)\ln(1-x)], \quad (4)$$

where w is the atomic exchange interaction parameter characterizing enthalpy of mixing, k_{B} is Boltzmann's constant, and Ω is the unit cell volume.

The gradient term of $\mathbf{P}$ in Eq. 1 characterizes the energy contribution associated with polarization change across domain walls and interphase interfaces, and the gradient term of x, which vanishes in compositionally homogeneous systems, characterizes the energy contribution from composition gradient across interfaces between phases of different compositions, where β_P and β_x are the corresponding gradient coefficients.

The $\mathbf{k}$-space integral in Eq. 1 gives the electrostatic energy of polarization distribution $\mathbf{P}(\mathbf{r})$ and the elastostatic energy of spontaneous strain distribution $\boldsymbol{\varepsilon}^0(\mathbf{r})$, where ε_0 is the permittivity of free space, $\mathbf{n} = \mathbf{k}/k$ is a directional unit vector in $\mathbf{k}$-space, $K_{ijkl} = C_{ijkl} - n_m C_{ijmn}\Omega_{np}C_{klpq}n_q$, $\Omega_{ik} = (C_{ijkl}n_jn_l)^{-1}$, C_{ijkl} is the elastic modulus tensor, the functions $\tilde{\mathbf{P}}(\mathbf{k})$ and $\tilde{\boldsymbol{\varepsilon}}^0(\mathbf{k})$ are the Fourier transform of the fields $\mathbf{P}(\mathbf{r})$ and $\boldsymbol{\varepsilon}^0(\mathbf{r})$, respectively, and the superscript asterisk * indicates the complex conjugate. The elastostatic energy is evaluated by using Khachaturyan's microelasticity theory of elastically homogeneous system [10], and elastic isotropy is assumed. In terms of Young's modulus E and Poisson's ratio v, the tensor K_{ijkl} becomes explicitly

$K_{ijkl} = Ev(1 - v^2)^{-1}(\delta_{ij}\delta_{kl} - \delta_{ij}n_kn_l - \delta_{kl}n_in_j) + 0.5E(1 + v)^{-1}(\delta_{ik}\delta_{jl} + \delta_{il}\delta_{jk} - \delta_{ik}n_jn_l - \delta_{il}n_jn_k - \delta_{jk}n_in_l - \delta_{jl}n_in_k) + E(1 - v^2)^{-1}n_in_jn_kn_l$. The spontaneous strain $\boldsymbol{\varepsilon}^0$ in ferroelectrics is a secondary order parameter and is coupled to the primary order parameter $\mathbf{P}$ through electrostriction coefficient tensor Q_{ijkl}, $\varepsilon^0_{ij} = Q_{ijkl}P_kP_l$, thus $\boldsymbol{\varepsilon}^0$ is not an independently evolving field variable.

The evolution of polarization and domain microstructure is characterized by the time-dependent Ginzburg–Landau equation [3–5]:

$$\frac{\partial \mathbf{P}(\mathbf{r},t)}{\partial t} = -L\frac{\delta F}{\delta \mathbf{P}(\mathbf{r},t)} + \boldsymbol{\xi}(\mathbf{r},t), \tag{5}$$

where L is the kinetic coefficient, and $\xi(\mathbf{r}, t)$ is Gaussian-distributed Langevin noise term that accounts for the effect of thermal fluctuation. The diffusional decomposition process is characterized by the Cahn-Hilliard nonlinear diffusion equation [11]:

$$\frac{\partial x(\mathbf{r},t)}{\partial t} = \nabla \cdot D\nabla\frac{\delta F}{\delta x(\mathbf{r},t)}, \tag{6}$$

where D is the chemical mobility of diffusion.

In computer simulations, material-specific parameters are used. In the case of $Pb(Zr_{1-x}Ti_x)O_3$, the coefficients of free energy density function, i.e., α_i, α_{ij}, and α_{ijk} in Eq. 3, are functions of temperature T and composition x as determined from experimental data [9]. For example, with composition $x = 0.5$ around morphotropic phase boundary, which is of our particular interest as discussed in the next section on inter-ferroelectric phase transformation, the coefficients at room temperature assume the following values [9]: $\alpha_1 = -2.67 \times 10^7$ m/F, $\alpha_{11} = -1.43 \times 10^7$ m^5/C^{2}F, $\alpha_{12} = 1.57 \times 10^7$ m^5/C^{2}F, $\alpha_{111} = 1.34 \times 10^8$ m^9/C^{4}F, $\alpha_{112} = 1.17 \times 10^9$ m^9/C^{4}F, and $\alpha_{123} = -4.77 \times 10^9$ m^9/C^{4}F. The gradient coefficients are $\beta_P = 0.4k_BT_Cl^2/\Omega P_0^2$ and $\beta_x = 0.8k_BT_Cl^2/\Omega$, where $T_C = 748$ K is Curie-Weiss temperature of $PbTiO_3$, $\Omega = 67 \times 10^{-30}$ m^3 is unit cell volume, $P_0 = 0.76$ C/m^2 is saturation polarization, and the computational mesh size is $l = 2$ nm. The parameter for enthalpy of mixing is $w = 0.5k_BT_C/\Omega$. Periodic boundary condition is employed to evaluate the Fourier transform by using fast Fourier transform algorithm.

Inter-ferroelectric phase transformations

Many ferroelectric materials exhibit more than one ferroelectric phases. Inter-ferroelectric phase transformation is a transformation between two ferroelectric phases of different crystallographic symmetries. Such a phase transformation can be caused by change in either temperature or composition. Examples of temperature-induced inter-ferroelectric phase transformations can be found in perovskite-type compounds, e.g., $BaTiO_3$ and $KNbO_3$. $BaTiO_3$ exhibits four phases depending on temperature: upon cooling, paraelectric cubic phase transforms to ferroelectric tetragonal phase at 120 °C, to ferroelectric orthorhombic phase at 5 °C, and to ferroelectric rhombohedral phase at −90 °C [12]. The high-temperature cubic → tetragonal transition is ferroelectric phase transformation, and the tetragonal ↔ orthorhombic and orthorhombic ↔ rhombohedral transitions at lower temperatures are inter-ferroelectric phase transformations. The temperature-induced phase transformation behavior of $KNbO_3$ is qualitatively similar to that of $BaTiO_3$ except all transformations occur at higher temperatures: ferroelectric cubic → tetragonal transformation at 435 °C, and inter-ferroelectric tetragonal ↔ orthorhombic and orthorhombic ↔ rhombohedral transformations at 225 °C and −10 °C, respectively [12].

Perovskite-type ferroelectric solid solutions provide examples of composition-induced inter-ferroelectric phase transformations, e.g., $Pb(Zr_{1-x}Ti_x)O_3$ (PZT) [13], $Pb[(Zn_{1/3}Nb_{2/3})_{1-x}Ti_x]O_3$ (PZN-PT) [14] and $Pb[(Mg_{1/3}Nb_{2/3})_{1-x}Ti_x]O_3$ (PMN-PT) [15]. These pseudo-binary solid solutions exhibit qualitatively similar temperature-composition phase diagrams: in addition to a paraelectric cubic phase above the composition-dependent Curie temperature, a nearly vertical (i.e., almost temperature-independent) morphotropic phase boundary (MPB) separates ferroelectric rhombohedral and tetragonal phases at low and high Ti contents, respectively. Inter-ferroelectric rhombohedral ↔ tetragonal transformation occurs across the MPB, which is located at composition $x = 0.48$, 0.10, and 0.34 in PZT, PZN-PT, and PMN-PT, respectively [13–15].

These perovskite-type ferroelectric compounds and solid solutions exhibit qualitatively similar thermodynamic behaviors in the following sense: there are two ferroelectric phases in the vicinity of inter-ferroelectric phase transformation temperature (e.g., $BaTiO_3$, $KNbO_3$) or composition (e.g., PZT, PZN-PT, PMN-PT), with small energy gap while large crystal lattice distortion between the two phases. The small energy gap between the two ferroelectric phases makes it possible to induce inter-ferroelectric phase transformation by external electric field, which allows us to exploit the large crystal lattice distortion strain associated with the field-induced inter-ferroelectric phase transformation.

Inter-ferroelectric phase transformations, as compared with phase transformation between high-symmetry paraelectric cubic phase and low-symmetry ferroelectric phase, offer two important advantages:

(1) The initial state of an inter-ferroelectric phase transformation is not a high-symmetry paraelectric cubic phase, which does not possess any domains; instead, the initial state is a low-symmetry ferroelectric phase

consisting of domain microstructures, which can be optimized by domain engineering.

(2) An inter-ferroelectric phase transformation involves two low-symmetry ferroelectric phases and, thus, a larger number of polar structural domain variants, which provides more degrees of freedom to control domain microstructure formation and evolution.

It is the kinetic pathway of domain evolution during inter-ferroelectric phase transformation that directly determines the macroscopic behaviors of ferroelectric materials. Both of the above advantageous features provide opportunities to engineer the initial domain microstructures and control the kinetic pathways of domain evolutions during field-induced inter-ferroelectric phase transformations to exploit the desired strain behaviors.

Crystallographic domain engineering

Ferroelectrics undergo displacive phase transformation upon cooling across Curie temperature. The primary thermodynamic variable (called long-range order parameter) that characterizes ferroelectric phase transition is spontaneous electric polarization. Development of spontaneous polarization is accompanied with a secondary effect of lattice distortion (a phenomenon called electrostriction), thus spontaneous strain is a secondary order parameter. Therefore, ferroelectrics are (secondarily) multiferroic.

Domains are essential feature of ferroelectrics. Development of spontaneous strain upon ferroelectric phase transition breaks the lattice symmetry of the parent phase and transforms the parent phase to lower-symmetry product phase. As permitted by the higher symmetry of the parent phase, several structural variants are produced, which are crystallographically equivalent but with different orientations as characterized by symmetry-related spontaneous strains. Formation of multiple structural variants within the same parent crystal lattice causes lattice misfit, generating elastic strain and stress and increasing elastostatic energy. Minimization of the elastostatic energy drives the evolution and formation of strain-accommodating, twin-related elastic domain microstructures. Simultaneously, development of spontaneous polarization produces several polar variants with dipole moment aligned along different (but equivalent) crystallographic directions (called easy axes). Formation of multiple polar variants causes electric charge accumulation, generating internal field and increasing electrostatic energy. Energy minimization drives the electric domains to evolve and form charge-accommodating, head-to-tail and/or reversal patterns. The intrinsic coupling between spontaneous polarization and strain in ferroelectrics leads to coupling between electric domains and elastic domains, resulting in formation of head-to-tail patterns of polarization within elastic structural domains, i.e., polar structural domains. Such domain microstructures simultaneously minimize electrostatic and elastostatic energies.

All polar structural domains will form with equal probabilities if no electric field is applied, since they are energetically degenerate. An externally applied electric field breaks the degeneracy and selects certain polar structural domains of energetically favorable orientations. In particular, a ferroelectric phase transformation under external electric field will nucleate polar domains of selected orientations, which subsequently grow and form domain microstructures of controlled configurations. For ferroelectric single crystals, the external electric field can be applied along specific crystallographic axis to engineer the domain microstructures. It is worth noting that experiments found that electric field applied along non-polar axes of ferroelectric single crystals produces desired domain microstructures and electromechanical properties [16, 17]. The obtained domain microstructures under non-polar electric field are called engineered domain configurations, and this technique is called crystallographic domain engineering.

Figure 1 shows computer simulation of domain microstructure evolution and formation under electric field. In particular, we consider cooling of ferroelectric single crystals across Curie temperature in external electric field applied along non-polar axes. Three generic cases are investigated (Wang et al. unpublished data):

(a) For stable ferroelectric rhombohedral phase, the polar directions are along ⟨111⟩ axes. Under electric field applied along non-polar [100] axis, ferroelectric phase transformation forms rhombohedral twins of (100) twin plane.

(b) For the same stable ferroelectric rhombohedral phase but under electric field applied along non-polar [110] axis, ferroelectric phase transformation forms rhombohedral twins of (110) twin plane.

(c) For stable ferroelectric tetragonal phase, the polar directions are along ⟨100⟩ axes. Under electric field applied along non-polar [111] axis, ferroelectric phase transformation forms tetragonal twins of (110) twin plane.

Our computer modeling and simulation demonstrates that application of electric field is an effective way to control the domain microstructure formation. Furthermore, the average domain sizes exhibit a systematic dependence on the magnitude of the electric field, as revealed by the simulation and shown in Fig. 2 (Wang et al. unpublished data). Control of domain patterns and domain sizes through thermo-electrical treatment in experiments has been reported [18]. The detailed mechanisms for crystallographic

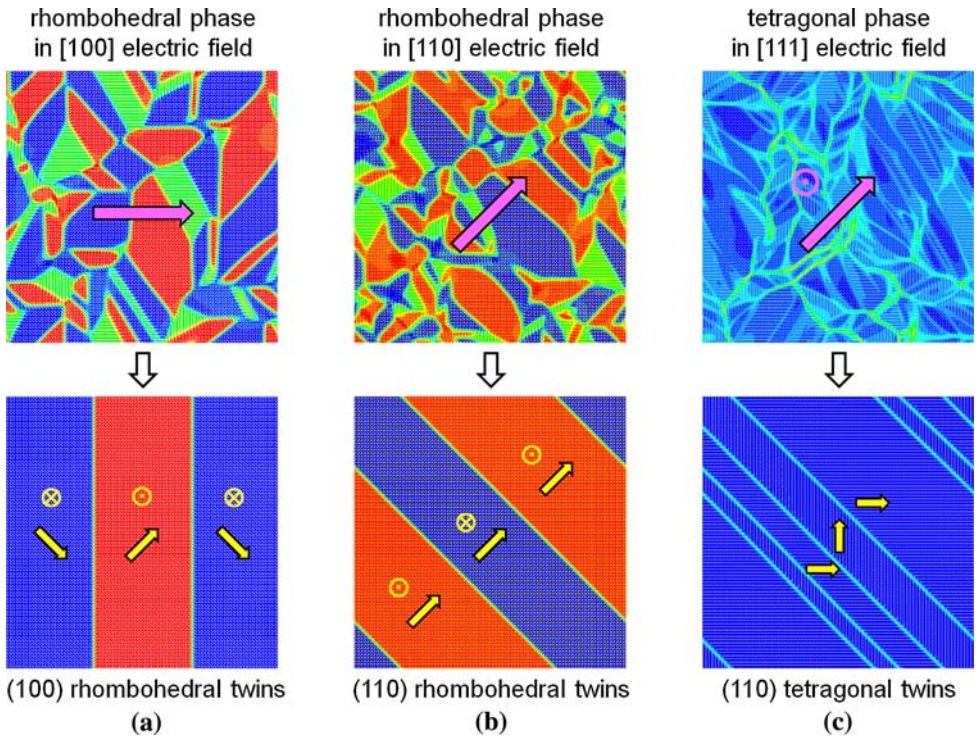

Fig. 1 (Color online) Computer simulation of domain evolution and twin formation in ferroelectric single crystals under electric field applied along non-polar axes during ferroelectric phase transformation (Wang et al. unpublished data). Different columns show different ferroelectric phases under different non-polar electric fields. *Top row* shows early-stage domain microstructures after cooling below Curie temperature. *Bottom row* shows fully developed engineered domain configurations consisting of structural twins and head-to-tail polarization patterns. *Purple arrows* in *top-row* figures represent electric field directions. *Yellow arrows* in *bottom-row* figures represent polarization directions in individual domains. Symbols ⊗ and ⊙ represent out-of-plane vector components, and in-plane components are represented by *arrows*

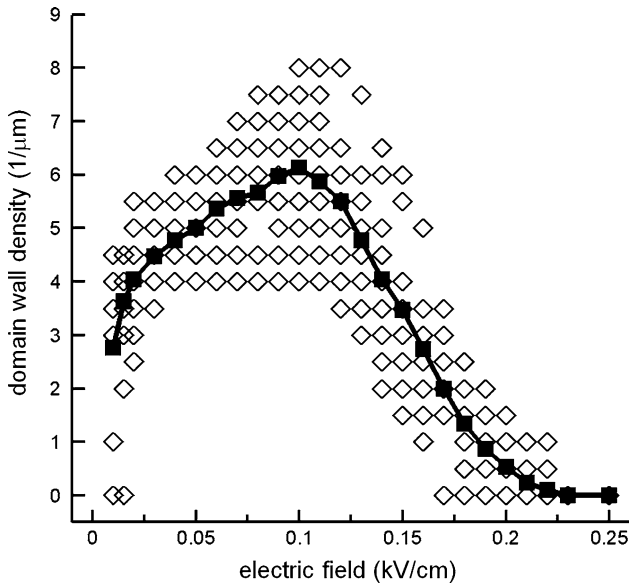

Fig. 2 Computer simulation of the dependence of average domain size (domain wall density) on the magnitude of electric field in crystallographic domain engineering (Wang et al. unpublished data). *Open symbols* represent individual simulation results. *Filled symbols* represent average results

domain engineering are currently investigated as our ongoing research and will be reported elsewhere (Wang et al. unpublished data). In the next section, we will show that such engineered domain configurations with controlled domain sizes provide the optimal initial domain microstructures for field-induced inter-ferroelectric phase transformations to exploit the desired strain behaviors.

Kinetic pathways and domain mechanisms

Domain wall broadening

Figure 3 shows computer simulation of domain microstructure evolution during field-induced inter-ferroelectric phase transformation in single crystal consisting of crystallographically engineered domain microstructure. As one example, we consider stable ferroelectric tetragonal phase consisting of (110) twins, as shown in Fig. 1c, which is obtained under electric field along non-polar [111] axis. If an external electric field is applied to this engineered domain microstructure along [100] direction, which is a polar axis of ferroelectric tetragonal phase, a conventional

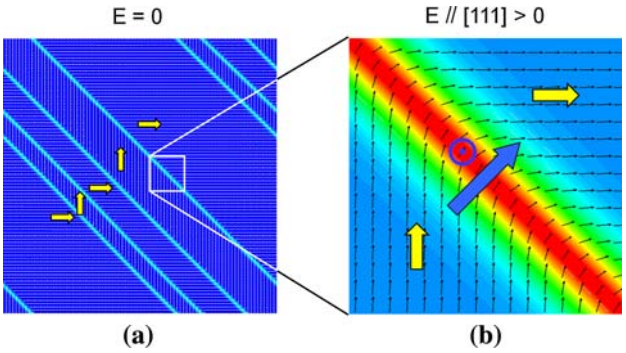

Fig. 3 (Color online) Computer simulation of heterogeneous nucleation and growth of metastable rhombohedral phase at domain walls of stable tetragonal phase during electric field-induced inter-ferroelectric phase transformation. **a** Crystallographically engineered domain microstructure as obtained in Fig. 1c. **b** Domain wall broadening under electric field applied along non-polar axis. *Yellow arrows* represent polarization directions in individual domains. *Blue arrow* and symbol ⊙ represent, respectively, in-plane and out-of-plane vector components of applied electric field

domain wall motion mechanism will operate, upon which [100] domains grow at the expense of [010] domains. This domain switching process would generate large strain, but is accompanied with hysteresis and/or is usually irreversible. In the simulation, instead of polar axis, an external electric field is applied along a non-polar axis, i.e., [111] direction. Since [111] is a polar axis of the metastable ferroelectric rhombohedral phase, the electric field induces an inter-ferroelectric phase transformation. It is important that the engineered domain microstructure shown in Fig. 3a, which is the same as in Fig. 1c, provides the optimal kinetic pathway for the [111]-field-induced inter-ferroelectric phase transformation to exhibit the desired large strain with low hysteresis and high reversibility. The inter-ferroelectric phase transformation proceeds through a heterogeneous-nucleation-and-growth process at domain wall region, reflected as a domain wall broadening phenomenon [19]. Because of the equal energy of tetragonal polar domains in [111] electric field, domain walls do not move, which eliminates the hysteresis associated with the irreversible wall motions. On the other hand, the domain walls serve as natural sites for heterogeneous nucleation of field-induced rhombohedral phase, which subsequently grow in response to increasing electric field. Since the domain walls behave like pre-existing embryos of the new phase, this process starts upon application of low field and gradually proceeds with increasing field. This enhances material response at low electric field regime. Also, since the rhombohedral phase is metastable, it reversibly transforms back to tetragonal phase with decreasing field. As a result, such a field-induced inter-ferroelectric phase transformation produces large, reversible and anhysteretic piezoelectric strain. Similar processes are expected for inter-ferroelectric phase transformations between other phases. The simulated reversible modification of domain wall structures help better understand the role of domain microstructures to exploit advanced properties of ferroelectric and piezoelectric materials.

Domain size effect

Since the piezoelectric contribution from field-induced inter-ferroelectric phase transformation through domain wall broadening mechanism is proportional to the domain wall density (i.e., reciprocal of average domain size) in the crystal, the piezoelectric coefficients should depend on the domain sizes. Such a domain size effect has been experimentally observed [18]. The important physical implication of the domain size effect is that ultrahigh piezoelectricity could be achieved with crystallographically engineered nanodomain microstructures, where nanodomains provide high domain wall density. It is worth noting that nanodomains are directly observed in ferroelectrics by transmission electron microscopy (TEM) in recent experiments, as discussed in the following section.

Nanodomains in morphotropic phase boundary ferroelectrics

Recent theoretical [20–26] and experimental [27–34] investigations reveal a new nanodomain aspect of perovskite-type ferroelectric solid solutions around the morphotropic phase boundaries. Combined TEM, convergent beam electron diffraction (CBED), and high-resolution electron microscopy (HREM) experiments directly observe nanotwins of tetragonal and rhombohedral phases with average size $\sim$10 nm in ferroelectric PMN-PT [27–30]. Nanodomains with typical sizes $\sim$10 nm are also observed in PZT by complementary TEM, CBED, electron paramagnetic resonance, and high-resolution synchrotron X-ray diffraction experiments [31–34]. These nanodomains appear as monoclinic phases in X-ray and neutron diffraction [35]. The crystallographic analysis reveals an adaptive nanotwin nature of these monoclinic phases, where the average structures of nanotwins resemble monoclinic phases [20–22]. The diffraction analysis shows that, due to the coherent scattering and interference effects peculiar to nanodomains, diffraction perceives the nanotwins as monoclinic phases [23, 24] (the induction of new monoclinic phase was suggested by the extraordinary diffraction peak patterns that otherwise cannot be explained by the conventional diffraction theory of coarse domains [36]). The thermodynamic analysis shows that drastically reduced domain wall energy around MPB leads to domain miniaturization to nanoscale [25, 26]. A direct correlation is established by experiments between the

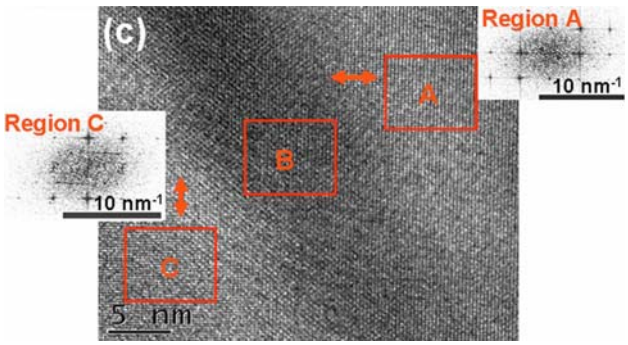

Fig. 4 (Color online) HREM observation of twin-related nanodomains (regions A and C) with broad domain walls (region B) in PMN-PT near MPB (reproduced with permission—Ref. [30]). Insets show the power spectrum (Fourier transform) obtained from regions A and C

TEM observed nanodomains and the extraordinary X-ray diffraction peak profiles in PZT [31, 33].

It is worth noting that HREM observes nanotwins with broad domain walls in PMN-PT near MPB, as shown in Fig. 4 [30], where a broad transition region (marked B) exists between two twin-related regions (marked A and C), which is similar to the simulated broadened domain walls shown in Fig. 3b. The domain size is $\sim$10 nm, and the domain wall thickness is $\sim$5 nm, which are comparable, indicating a significant volume fraction of the nanodomained ferroelectric material in transitional domain wall regions. Clearly, domain walls play an important role in ferroelectrics, especially with nanodomain microstructures.

Formation of nanodomains depends on compositions and is observed near MPBs [27–36]. Since the best piezoelectric properties are also obtained at compositions around MPBs [13–15, 37, 38], the relations between nanodomains and piezoelectric properties are interesting issues. It is noteworthy that the largest piezoelectric strain is also obtained along a non-polar axis and exhibits high reversibility and small hysteresis, which is attributed to crystallographically engineered domain configuration [16]. These experimental observations [13–15, 27–38] show that nanodomain microstructures and mechanisms are important issues in studying the piezoelectric properties of ferroelectrics.

Phase-coexisting domain microstructures

Phase coexistence is commonly observed around MPBs in ferroelectric solid solutions [39–42]. Because the best piezoelectric properties are obtained around MPBs, the effect of phase coexistence on the piezoelectric properties is also an interesting question. Our computer modeling and simulation shows that domains play a significant role in the phase coexistence phenomenon [43]. It is found that minor domains of metastable phase spontaneously coexist with and bridge major domains of stable phase in compositionally homogeneous systems. Such phase-coexisting mosaic domain microstructures effectively reduce elastostatic and electrostatic energies in complex domain microstructures, which arise from the frustrations caused by the crystal lattice misfit among multiple structural orientation variants and the polarization distribution among multiple polar axes. Similar phase coexistence phenomenon is also observed in computer simulation of epitaxially strained ferroelectric thin films [44]. Since the phase-coexisting domain microstructure corresponds to a minimum energy state, domain evolution away from this state as induced by external field has a tendency of automatic recovery, providing desired reversibility. This generates a ferroelectric shape memory effect. The simulation also shows a grain size effect of phase coexistence [2], where the width of phase coexistence composition range increases with decreasing grain sizes. This is caused by the internal mechanical and electric boundary conditions imposed at grain boundaries, which affect the phase-coexisting domain microstructures more significantly in smaller grains, giving rise to the grain size effect. Thus, grain size is one control parameter to tailor the piezoelectric properties. The spontaneous coexistence of minor domains of metastable phase with major domains of stable phase also provides an easy kinetic pathway for interferroelectric phase transformation due to the pre-existing metastable phase.

The presence of MPB as a sharp-line phase boundary violates Gibbs phase rule for thermodynamically equilibrium temperature-composition phase diagram [7, 26]. As a result, the compositional degree of freedom leads to phase decomposition and formation of phase-coexisting domain microstructures. Our computer modeling and simulation shows formation of nanoscale lamellar domains of coexisting phases of different compositions [6]. Unlike the bridging domains of coexisting phases of homogeneous composition [2, 43], the composition heterogeneity defines phase distribution and confines the displacive phase transformation and domain switching. Such a compositionally heterogeneous ferroelectric system is expected to exhibit unique behaviors, similar to the anhysteretic response associated with confined displacive phase transformation found in compositionally heterogeneous alloys [45]. Simulation study of piezoelectric properties of compositionally heterogeneous ferroelectrics is under way. To control the composition profile, temperature and cooling rate are processing parameters.

Working principles

Based on above-discussed computational [2, 6, 19, 43, Wang et al. unpublished data], theoretical [7, 20–26], and

experimental [16–18, 27–36] findings, some fundamental principles and domain mechanisms can be systematized. Synergistic operations of these thermodynamic and kinetic principles are essential to achieve uniquely combined properties of large, reversible and anhysteretic strain behavior. These working principles are:

(I) *Field-induced inter-ferroelectric structural phase transformation to achieve large strain.*
(II) *Field-induced stable-metastable phase transformation to maximize reversibility.*
(III) *Heterogeneous nucleation-and-growth process at domain walls to enhance low-field responses.*
(IV) *Deactivation of domain wall motion by applying external fields along nonpolar axes to minimize hysteresis.*
(V) *Domain wall broadening mechanism and domain size effect to exploit nanoscale engineered domain microstructures.*
(VI) *Bridging domain mechanism and phase coexistence to promote ferroelectric shape memory effects.*

In order for these principles to work together without compromising one another, special domain microstructures and evolution kinetic pathways are required, which can be achieved by crystallographic domain engineering technique. In particular, to exploit the useful large strain of crystallographic phase transformation and at the same time eliminate the detrimental hysteresis and irreversibility as usually associated with the transformation, field-induced stable-metastable inter-ferroelectric phase transformation is preferred. To eliminate the nucleation barrier to stable-metastable phase transformation that causes hysteresis, heterogeneous nucleation and growth at domain walls provide the desired kinetic pathways. The non-polar direction of applied field not only favors the metastable phase, but also provides zero driving force to the movement of domain walls of stable phase, thus deactivating domain wall motion and eliminating the associated energy dissipation without reducing inter-phase interface mobility (note that doping, as often employed to pin domain walls and minimize hysteresis, impedes the movement of inter-phase interfaces, thus is detrimental to the desired inter-ferroelectric phase transformation). Therefore, the crystallographically engineered domain microstructures make possible synergistic operations of multiple working principles, and achievable unique combination of large, reversible and anhysteretic strain attributes.

Implications to other inter-ferroic phase transformations

The working principles discussed above for inter-ferroelectric phase transformation also provide insights into the strain behaviors of other ferroic and multiferroic materials, such as conventional and magnetic shape memory alloys and giant magnetostrictive materials. Ferroic crystals undergo displacive phase transformations upon temperature change. According to the primary thermodynamic variables (long-range order parameters) that characterize the phase transitions, ferroic materials are classified into three groups of distinct physical natures, namely, ferroelectrics, ferromagnetics, and ferroelastics, whose primary order parameters are spontaneous electric polarization, magnetization, and lattice strain, respectively. While apparently different, these three groups of ferroic materials are fundamentally interrelated with important commonalities among the underlying physical phenomena, where domain processes play central roles.

As examples, Terfenol-D [46] and Nitinol [47] are leading magnetostrictive material and shape memory alloy, respectively, and Ni–Mn–Ga [48] is a best studied magnetic shape memory alloy, each of which exhibits best field-induced strain properties of its own class. Inter-ferroic phase transformations occur in these materials, i.e., inter-ferromagnetic (ferrimagnetic) transformation in Terfenol-D [49], and inter-martensitic transformations in Nitinol [47] and Ni–Mn–Ga [48, 50], with coexistence of two or more ferroic phases and small energy gap between them [50–52]. These situations are similar to those discussed above for ferroelectrics.

Therefore, the gained understanding of thermodynamic and kinetic principles has general implications to displacive phase transformations and is helpful for design of new functional materials with advanced field-induced strain properties.

Insights learned from phase field modeling and simulation

This study discusses some new insights into the domain microstructures and mechanisms in high-performance piezoelectric materials learned from phase field modeling and simulation. The above discussed computational results demonstrate the efficacy of the phase field approach in investigating these phenomena, where insights have also been obtained based on experimental and theoretical findings. In the following, we briefly summarize our new insights in relation to the ones gained through other considerations.

Phase coexistence around morphotropic phase boundary has been commonly observed in experiments. It has been long-recognized that a two-phase zone is required around MPB, and the MPB is considered as located at the composition where the two phases coexist in equal quantity [13]. The origin of phase coexistence has been a topic of

many investigations, and insights have been gained from different perspectives, for example, stability and metastability of coexisting phases [42], solubility gap [39], compositional fluctuation [40], statistical distribution of accessible polar states [41], and equilibrium phase diagram satisfying Gibbs phase rule [7]. While these studies together provide a broad aspect of MPB phase coexistence phenomenon, none of them considers the formation of ferroelectric and ferroelastic domain microstructures and its role in phase coexistence. That is, the domain microstructure-dependent long-range electrostatic and elastostatic interactions are not considered. The phase field modeling and simulation reveals a bridging domain mechanism around MPB, where, as a result of electrostatic and elastostatic interactions, major and minor phases spontaneously coexist and form mosaic domain microstructures, while compositional inhomogeneity is not necessarily involved [43]; furthermore, it is found that phase coexistence depends on grain sizes, where grain boundaries impose internal mechanical and electric boundary conditions affecting the phase-coexisting domain microstructures in the grains [2].

Crystallographic domain engineering technique is first established by experiments, where ferroelectric single crystals with engineered domain configurations are found to exhibit drastically enhanced piezoelectric responses along non-polar axes [16, 17]. Subsequent experiments further observe a domain size effect, where the piezoelectric properties are found to significantly increase with decreasing domain sizes [18]. The enhanced property along non-polar direction has been attributed to the intrinsic piezoelectric anisotropy as calculated from single-domain crystals [17, 53, 54], which, however, only accounts for a small part of the experimentally measured property enhancement while does not explain the domain size effect. The phase field modeling and simulation results presented in Figs. 1, 2, and 3 explain these experimental findings [16–18] through domain microstructures and mechanisms, i.e., control of twin-related lamellar domains with different twin planes and domain sizes under external electric field of different directions and different strengths (Wang et al. unpublished data), and domain wall broadening under electric field along non-polar axis [19].

It is noteworthy that the origins of the abnormally high piezoelectric response near morphotropic phase boundaries and the enhanced piezoelectric response along non-polar axes remain a topic of active discussion and debate. As competing theories, it has been attributed to polarization rotation [55] and monoclinic phases [35], which focus on intrinsic contribution. Discussion of the intrinsic factors influencing the piezoelectric behaviors of PZT and morphotropic phase boundary phenomena, including polarization rotation and monoclinic phases based on first-principle calculations and thermodynamic analysis and relevant experimental observations, can be found in a recent review [56]. In particular, the thermodynamic analysis is based on the same Landau–Ginzburg–Devonshire theory as used in the phase field model, however, only single-domain state, thus, intrinsic contribution, is considered. The phase field model also takes into account multi-domain state, long-range electrostatic and elastostatic interactions, and extrinsic domain mechanisms. It is worth noting a recent review [57] of the experimental data on the piezoelectric response of thin film PZT for microelectromechanical systems (MEMS), where the domain microstructures and mechanisms, the effects of crystallographic orientation, composition, grain size, film thickness, mechanical boundary condition imposed by substrate, and, especially, the importance of morphotropic phase boundary are discussed.

Acknowledgements Support from National Science Foundation under Grant No. DMR-0705947 is acknowledged. The parallel computer simulations were performed on System X at Virginia Tech and Lonestar at Texas Advanced Computing Center.

References

1. Jin YM, Artemev A, Khachaturyan AG (2001) Acta Mater 49:2309
2. Rao WF, Wang YU (2008) Appl Phys Lett 92:102905
3. Semenovskaya S, Khachaturyan AG (1998) J Appl Phys 83:5125
4. Semenovskaya S, Khachaturyan AG (1998) Ferroelectrics 206–207:157
5. Li YL, Hu SY, Liu ZK, Chen LQ (2001) Appl Phys Lett 78:3878
6. Rao WF, Wang YU (2007) Appl Phys Lett 91:052901
7. Rossetti GA Jr, Zhang W, Khachaturyan AG (2006) Appl Phys Lett 88:072912
8. Devonshire AF (1949) Philos Mag 40:1040
9. Amin A, Haun MJ, Badger B, McKinstry H, Cross LE (1985) Ferroelectrics 65:107
10. Khachaturyan AG (1983) Theory of structural transformations in solids. John Wiley & Sons, New York, p 198
11. Cahn JW, Hilliard JE (1958) J Chem Phys 28:258
12. Jona F, Shirane G (1962) Ferroelectric crystals. Pergamon Press, Oxford, pp 108, 221
13. Jaffe B, Cook WR, Jaffe H (1971) Piezoelectric ceramics. London, Academic Press
14. Kuwata J, Uchino K, Nomura S (1981) Ferroelectrics 37:579
15. Choi SW, Shrout TR, Jang SJ, Bhalla AS (1989) Ferroelectrics 100:29
16. Park SE, Shrout TR (1997) J Appl Phys 82:1804
17. Park SE, Wada S, Cross LE, Shrout TR (1999) J Appl Phys 86:2746
18. Wada S, Yako K, Kakemoto H, Tsurumi T, Kiguchi T (2005) J Appl Phys 98:014109
19. Rao WF, Wang YU (2007) Appl Phys Lett 90:041915
20. Jin YM, Wang YU, Khachaturyan AG, Li JF, Viehland D (2003) Phys Rev Lett 91:197601
21. Jin YM, Wang YU, Khachaturyan AG, Li JF, Viehland D (2003) J Appl Phys 94:3629
22. Wang YU (2006) Phys Rev B 73:014113
23. Wang YU (2006) Phys Rev B 74:104109
24. Wang YU (2007) Phys Rev B 76:024108

25. Rossetti GA Jr, Khachaturyan AG (2007) Appl Phys Lett 91:072909
26. Rossetti GA Jr, Khachaturyan AG, Akcay G, Ni Y (2008) J Appl Phys 103:114113
27. Wang H, Zhu J, Lu N, Bokov AA, Ye ZG, Zhang XW (2006) Appl Phys Lett 89:042908
28. Wang H, Zhu J, Zhang XW, Tang YX, Luo HS (2008) Appl Phys Lett 92:132906
29. Wang H, Zhu J, Zhang XW, Tang YX, Luo HS (2008) J Am Ceram Soc 91:2382
30. Bhattacharyya S, Jinschek JR, Cao H, Wang YU, Li J, Viehland D (2008) Appl Phys Lett 92:142904
31. Schönau KA, Schmitt LA, Knapp M, Fuess H, Eichel RA, Kungl H, Hoffmann MJ (2007) Phys Rev B 75:184117
32. Schönau KA, Knapp M, Kungl H, Hoffmann MJ, Fuess H (2007) Phys Rev B 76:144112
33. Theissmann R, Schmitt LA, Kling J, Schierholz R, Schönau KA, Fuess H, Knapp M, Kungl H, Hoffmann MJ (2007) J Appl Phys 102:024111
34. Schmitt LA, Schönau KA, Theissmann R, Fuess H, Kungl H, Hoffmann MJ (2007) J Appl Phys 101:074107
35. Noheda B, Cox DE (2006) Phase Transitions 79:5
36. Noheda B, Cox DE, Shirane G, Gonzalo JA, Cross LE, Park SE (1999) Appl Phys Lett 74:2059
37. Kuwata J, Uchino K, Nomura S (1982) Jpn J Appl Phys 21:1298
38. Shrout TR, Chang ZP, Kim N, Markgraf S (1990) Ferroelectrics Lett 12:63
39. Benguigui L (1972) Solid State Commun 11:825
40. Kakegawa K, Mohri J, Shirasaki S, Takahashi K (1982) J Am Ceram Soc 65:515
41. Cao W, Cross LE (1993) Phys Rev B 47:4825
42. Isupov VA (2002) Ferroelectrics 266:91
43. Rao WF, Wang YU (2007) Appl Phys Lett 90:182906
44. Li YL, Chen LQ (2006) Appl Phys Lett 88:072905
45. Ni Y, Jin YM, Khachaturyan AG (2008) Metall Mater Trans A 39:1658
46. Clark AE (1980) In: Wohlfarth EP (ed) Ferromagnetic materials, vol 1. North-Holland, Amsterdam, p 531
47. Saburi T (1998) In: Otsuka K, Wayman CM (eds) Shape memory materials. Cambridge University Press, Cambridge, p 49
48. Chernenko VA, Segui C, Cesari E, Pons J, Kokorin VV (1998) Phys Rev B 57:2659
49. Newnham RE (1998) Acta Crystallogr A 54:729
50. Chernenko VA, Cesari E, Khovailo V, Pons J, Segui C, Takagi T (2005) J Magn Magn Mater 290–291:871
51. Holden AP, Lord DG, Grundy PJ (1996) J Appl Phys 79:4650
52. Ren X, Miura N, Zhang J, Otsuka K, Tanaka K, Koiwa M, Suzuki T, Chumlyakov Y, Asai M (2001) Mater Sci Eng A 312:196
53. Wada S, Muraoka K, Kakemoto H, Tsurumi T, Kumagai H (2004) Jpn J Appl Phys 43:6692
54. Damjanovic D (2005) J Am Ceram Soc 88:2663
55. Fu H, Cohen RE (2000) Nature 403:281
56. Bell AJ (2006) J Mater Sci 41:13. doi:10.1007/s10853-005-5913-9
57. Trolier-McKinstry S, Muralt P (2004) J Electroceram 12:7